RSC Advances

PAPER

View Article Online
View Journal | View Issue

Cite this: *RSC Adv.*, 2018, **8**, 9327

11-Mercaptoundecanoic acid capped gold nanoclusters as a fluorescent probe for specific detection of folic acid *via* a ratiometric fluorescence strategy†

Lei Meng,[ab] Jian-Hang Yin,[a] Yaqing Yuan[a] and Na Xu*[a]

A novel ratiometric fluorescence strategy is developed for specific detection of folic acid (FA) by using 11-mercaptoundecanoic acid protected gold nanoclusters (AuNCs@MUA). In this design, the fluorescence color of the probe can be switched among red, pink, violet and blue by varying the concentration of FA. AuNCs@MUA possesses strong fluorescence peaking at 612 nm (R-signal) and FA exhibits blue emissive auto-fluorescence at 446 nm (B-signal), showing a large emission shift of ~170 nm. When AuNCs@MUA approaches FA through electrostatic binding, the R-signal decreases while the B-signal increases with titration of FA. Based on the above phenomenon, a radiometric analysis platform is constructed for FA target detection, with a wide linear response range from 0 to 20 μM, and an excellent detection limit of 26 nM. This new ratiometric strategy exhibits low background, and wide signal changes in a low concentration range, which presents obvious advantages over most previous FA detections based on single-responsive fluorescence methods. Furthermore, the proposed method is successfully applied to determine FA in human serum samples.

Received 17th January 2018
Accepted 24th February 2018

DOI: 10.1039/c8ra00481a

rsc.li/rsc-advances

1. Introduction

Folic acid (FA) is important to human health, and is a water soluble compound of the vitamin B family and participates in a series of physiological processes.[1–4] FA is involved in the formation of red blood cells, as well as the acquisition, transport and enzymatic processing of one carbon unit for amino acid and nucleic acid metabolism.[5,6] Meanwhile, many reports have demonstrated that FA and vitamin B_{12} play essential roles in the synthesis of DNA and RNA.[7] The lack of FA gives rise to gigantocytic anemia, leukopenia, mental health issues, psychosis and other diseases.[8] So far, various methods such as high performance liquid chromatography (HPLC),[9–11] capillary electrophoresis (CE),[12] surface-enhanced Raman scattering (SERS),[13,14] and enzyme-linked immunosorbent assays (ELISA),[7,15] electrochemiluminescence (ECL) and photoelectrochemical (PEC) methods[16,17] have been applied to FA detection. However, majority of these methods are either of time-consuming, laborious, and requiring expensive facilities. Comparatively, fluorescence method has proved to be a more powerful optical technique for trace detection of FA.

To date, considerable information on fluorescence FA probes has been reported, where titration of FA can largely change fluorescence intensity of these probes. For example, the fluorescence of dendrimer encapsulated CdS quantum dots (QDs) could be greatly quenched by FA.[18] Similar FA induced fluorescence quenching phenomena have been observed in other probes such as N-doped carbon QDs,[19] layered double hydroxides (LDHs),[20] molecularly imprinted polymers (MIPs)[21] and nanoclusters (NCs).[22,23] Besides, Kamla Rawat *et al.* found that ZnSe and ZnSe@ZnS QDs could determine FA *via* fluorescence enhancement.[24] Nonetheless, these reported probes are totally based on one-single fluorescence response, which are easily interfered by many factors, such as instrumental parameters, microenvironment impact, concentration of sensors and photobleaching, *etc.* Ratiometric fluorescent sensors can overcome these problems, which rely on analyte-induced changes in the intensity of two or more emission bands and reflect the special characteristic of self-calibration. Recently, S. Chakravarty *et al.* developed polyvinyl alcohol stabilized CdTe QDs to determine FA with dual-emission fluorescence.[25] However, this fluorescence probe suffers from many drawbacks, such as toxic materials, tedious fabrication, phototoxicity, and poor sensitivity.

Herein, FA quenches the fluorescence of AuNCs@MUA at 612 nm *via* formation of ground state complex, while auto-fluorescence of FA at 446 nm can be increased linearly with titration of FA. Thereby the platform respectively shows dual

[a]*College of Materials Science and Engineering, Jilin Institute of Chemical Technology, Jilin 132022, China. E-mail: xn_1216@163.com*

[b]*College of Sciences, Jilin Institute of Chemical Technology, Jilin 132022, China*

† Electronic supplementary information (ESI) available. See DOI: 10.1039/c8ra00481a

emission peaks at 612 nm and 446 nm upon excitation by single-wavelength, and the fluorescence intensity ratio I_{446}/I_{612} can be served to detect FA. In this work, AuNCs@MUA possesses many advantages over previous FA fluorescence probes. Firstly, the fluorescence spectra of many reported FA probes always overlap or even merge that of FA mentioned above, where the optical properties of these probes such as fluorescence intensity and position will be interfered by auto-fluorescence of FA (see in Table S1†). Whereas, the emission peak of AuNCs@MUA at 612 nm is far away from that of FA, where the red emission (R-signal) response is only influenced by unique interaction between AuNCs@MUA and FA. Additionally, excitation and absorbance spectra of AuNCs@MUA exist in the deep ultraviolet region, excluding some other interferences such as inner filter effect and fluorescence resonance energy transfer. Finally, fluorescence for FA detection at long wavelength (~600 nm) has many advantages including effective tissue depth penetration, imaging sensitivity and non-invasivity, and good signal to background noise ratio. Thus, the proposed ratiometric strategy based on AuNCs@MUA appears to be a promising alternative for efficient and rapid detection of FA.

2. Experimental

2.1 Chemicals and materials

Hydrogen tetrachloroaurate trihydrate ($HAuCl_4 \cdot 3H_2O$), folic acid (FA), 11-mercaptoundecanoic acid (MUA) and trichloroacetic acid were obtained from Aladdin Reagent Co., Ltd. (Shanghai, China). Bovine serum albumin (BSA, fraction V) and amino acids (Ile, Pro, Arg, Gly, Gln, Ser, Ala, Leu, His) were purchased from Beijing Dingguo Changsheng Biotech Co. (Beijing, China). Other routine reagents like HCl, NaOH, NaCl, KCl, $MgCl_2$, $CaCl_2$, Na_2CO_3, $NaHCO_3$, NaH_2PO_4, Na_2HPO_4 and Na_3PO_4 were purchased from Tianjin Guangfu Fine Chemical Research Institute (Tianjin, China). All chemicals were of analytical reagent grade and were used without further purification. The water used throughout all the experiments was purified through a Millipore system.

2.2 Apparatus

Transmission electron microscopy (TEM) measurements were carried out by using a Tecnai F20 transmission electron microscope (FEI, USA). Dynamic light scattering (DLS) and zeta potential measurements were performed using a nano ZS90 laser scattering particles size and zeta-potential analyzer (Malvern, UK). The fluorescence intensity (FL) spectra were recorded by a LS-55 Luminescence Spectrometer (Perkin-Elmer, UK). UV-Vis absorbance spectra were tested by a Lambda 950UV/Vis/NIR instrument (PerkinElmer, UK). Fourier transform infrared (FTIR) spectra were collected with a Spectrum Two spectrometer (PerkinElmer, UK). The pH values were measured with FE 20 pH meter (Mettler-Toledo, China).

2.3 Synthesis of AuNCs@MUA

AuNCs were synthesized with MUA as template mainly according to the previous report,[26] but minor modification. Briefly, 500 μL $HAuCl_4$ (10 mM) was dissolved in the solution that was prepared by 100 μL NaOH (1 M) and 6.6 mg MUA to 10 mL ultrapure water. The mixture was stirring for 5 h at room temperature during which the colorless solution slowly turned pale yellow. Finally, the as-obtained products were purified by centrifugation (10 000 rpm, 20 min) to remove excess reactants containing the free MUA and gold ions. The purified AuNCs@MUA contained solution and the relevant freeze-drying powder was stored at 4 °C prior to use.

2.4 Detection of FA

The as-prepared AuNCs@MUA were dissolved in a Tris buffer solution (pH 8.0) to get a concentration of 10 μM (in terms of Au) containing various concentrations of FA. The solution was mixed thoroughly for 1 min at room temperature. The fluorescence spectra were then recorded in the wavelength range 400–700 nm with excitation at 340 nm. The ratio changes of the fluorescence intensities (I_{446}/I_{612}) were used to construct the curves and evaluate the performance of AuNCs@MUA toward FA. The selectivity of this sensing system for FA activity was assessed by using other substances as K^+, Na^+, Mg^{2+}, Ca^{2+}, Cl^-, CO_3^{2-}, HCO_3^-, PO_4^{3-}, HPO_4^{2-}, $H_2PO_4^-$, BSA, glucose and amino acids. All the measurements are performed at ambient conditions.

2.5 Real sample test

Drug-free human whole blood samples were obtained from healthy volunteers at early morning time. The blood samples were centrifuged at 5000 rpm for 10 min after standing for 2 h at room temperature, and the supernatant was added NaOH and $ZnSO_4$ as protein precipitant and decolorizer to eliminate the interferences. After vortexing for 1 min, the mixture was centrifuged at 10 000 rpm for 10 min. Then the obtained upper plasma was transferred to a new tube and diluted by 100 times with ultrapure water and stored at 4 °C for further analyzing. FA with different concentrations were introduced into the diluted plasma samples to prepare the spiked samples.[27,28] Human blood serum samples were obtained from Medical College of Beihua University, China, and all analyses were performed at the Nanotechnology & Application Laboratory. All experiments were performed in compliance with the relevant laws and national guidelines (Ethical Guidelines for Biomedical Research on Human Participants, provided by China National Health and Family Planning commission), and the ethical clearance for the same was provided by the Medical College of Beihua University, Jilin City. All the experiments with the samples were performed with informed consent obtained from the persons who provided the samples.

3. Results and discussion

3.1 Synthesis and characterization of AuNCs@MUA

As-synthesized AuNCs@MUA in this work are prepared according to one-pot reduction method by using $NaBH_4$. The TEM image in Fig. 1a reveals that resulted particles are well dispersed, and size distribution obtained by DLS demonstrates

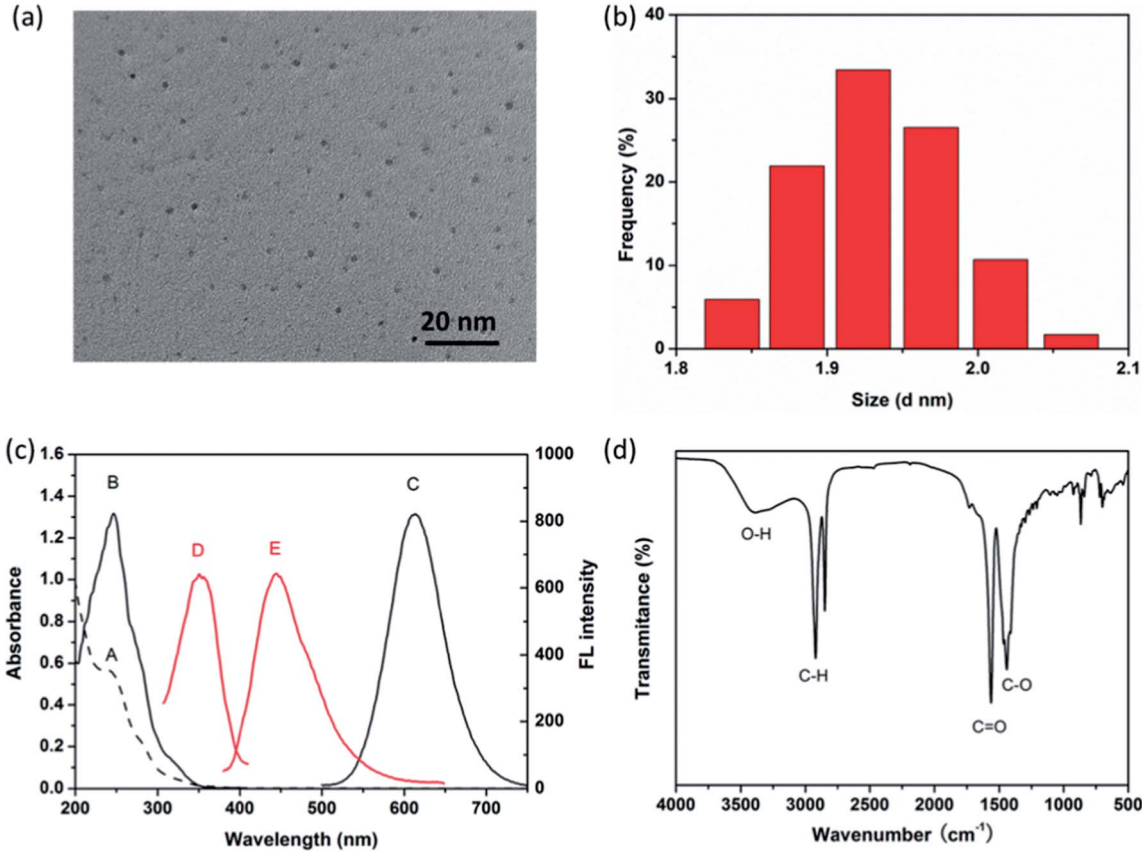

Fig. 1 (a) TEM image and (b) size distribution of as-synthesized AuNCs@MUA. (c) The UV-Vis absorption spectrum (A), photoexcitation (B) and photoemission (C) of AuNCs@MUA, photoexcitation (D) and photoemission (E) of FA. (d) FTIR spectrum of AuNCs@MUA.

the average diameter is 1.9 ± 0.2 nm (Fig. 1b), suggesting MUA capped Au nanoclusters but not nanoparticles are successfully prepared.[29] Fig. 1c shows optical properties of the products such as UV-Vis absorption (dash curve), fluorescence excitation and emission (solid curve) spectra. Two well-defined absorption bands can be observed at 243 nm and 280 nm in UV-Vis spectrum, ascribed to the interband electronic transitions of AuNCs.[30] In addition, absorption feature shows no surface plasmon resonance (SPR) band at around 500–600 nm, indicating absence of large Au nanoparticles.[31] The maximum fluorescence excitation and emission wavelengths of AuNCs@MUA are peaking at 280 and 612 nm, respectively. In contrast, the emission spectrum of FA shows a fluorescence peak centered at 446 nm when exited by 352 nm (see in red curve of Fig. 1c). Combined with UV-Vis studies, it can be confirmed that the fluorescence properties of AuNCs@MUA and FA should be "isolated", where they will not interact with each other through inner filter effect (IFE) or fluorescence resonance energy transfer (FRET) during process of FA detection.[32,33] Thereby, unique optical properties offer AuNCs@MUA ability to monitor FA by using dual-emission fluorescence. Specifically, although BSA stabilized AuNCs (AuNCs@BSA) with red emission have been also used as a probe to determine FA and some conditions of experiments reported are even similar to us, such dual-emission phenomenon has not been noticed and mentioned in these reports.[22,23] As for FTIR spectrum (Fig. 1d), five characteristic peaks of AuNCs@MUA were observed at 3400 cm^{-1} (O–H), 2920 and 2850 cm^{-1} (C–H), 1570 cm^{-1} (C=O) and 1440 cm^{-1} (C–O). Based on these FTIR results, it assumed that the AuNCs@MUA are terminated by amounts of carboxyl (–COOH) groups.[34]

3.2 Principle of detecting FA by using AuNCs@MUA

As shown in Fig. 2a, 20 μM FA is added into the aqueous solution contained 10 μM AuNCs@MUA. It is found that introduction of FA results in 82% fluorescence quenching of AuNCs@MUA, while a new fluorescence corresponding to FA emerges simultaneously. Interestingly, both emission spectra of AuNCs@MUA and FA reveal red-shift for the AuNCs@MUA-FA mixture, suggesting that changed microstructure of AuNCs@MUA occurs as FA attaches to the surface. In addition, absorbance spectra of AuNCs@MUA are entirely different in absence and presence of FA. Fig. 2b shows two new bands at 276 nm and 238 nm appear in AuNCs@MUA-FA mixture, indicating fluorescence quenching may belong to static one upon formation of the ground state complex (Scheme 1). Besides, Fig. S1† reveals that the fluorescence intensity has been decreased linearly with increasing FA's concentration. It is found that fitting line from quenching data consists well with Stern–Volmer equation[35]

$$\frac{I_0}{I} = 1 + K_{sv}[FA], \quad (1)$$

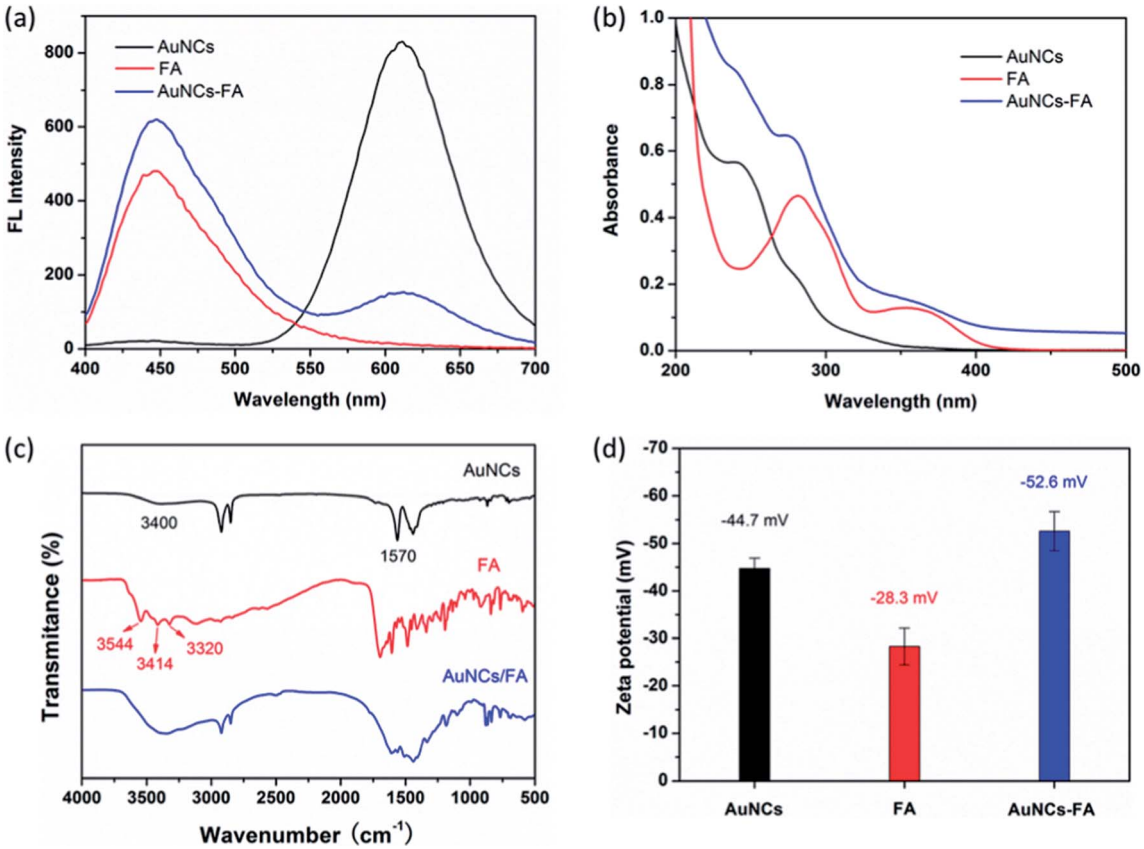

Fig. 2 (a) Fluorescence spectra, (b) absorbance spectra, (c) FTIR spectra and (d) zeta potentials of bare AuNCs@MUA (black), bare FA (red) and AuNCs@MUA-FA mixture (blue).

and quenching constant (K_{sv}) is calculated to be 5.9×10^4 M^{-1}. To further confirm this principle, FTIR spectra, DLS and zeta potentials have been employed to access the binding between AuNCs@MUA and FA. According to previous characterization of AuNCs@MUA (Fig. 1d), the typical bands at 3400 cm^{-1} (O–H) and 1570 cm^{-1} (C=O) are assigned to stretching vibrations of –COOH groups (Fig. 2c). In presence of FA, the band for O–H shows blue shift while that for C=O becomes week. Contrastively, the bands of FA at 3544 cm^{-1} and 3414 cm^{-1} are respectively assigned to ring –OH and $-NH_2$ groups,[36] which have been vanished in AuNCs@MUA-FA mixture. These spectral changes indicate that the –COOH groups of AuNCs@MUA and $-NH_2$ of FA take part in the conjugation. Meanwhile, zeta potential investigation is carried out to study surface chemical features, as shown in Fig. 2d. It is found that zeta potentials of AuNCs@MUA and FA are −44.7 mV, −28.3 mV, respectively. Negative surface charge for these two species is possible attributed to deprotonation of –COOH groups. As for AuNCs@MUA-FA mixture, the zeta potential is −52.6 mV, which is higher than the sum of two zeta potentials mentioned above. The special variation possibly results from the electrostatic binding between negatively charged –COOH and positive

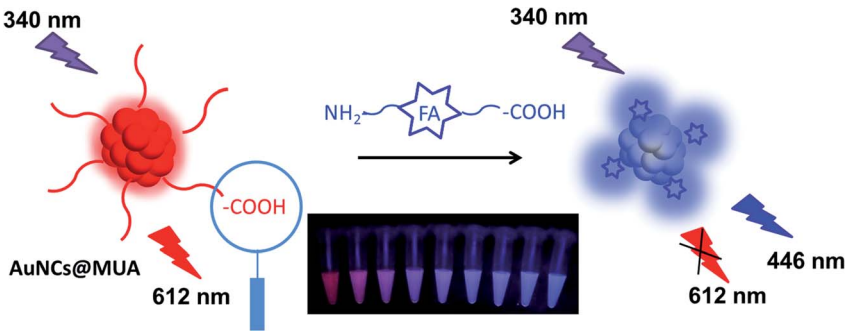

Scheme 1 Schematic illustration for ratiometric detection of FA based on static quenching *via* formation of ground state complex.

charged $-NH_2$ in AuNCs@MUA-FA mixture. As shown in Fig. S2,† grain size of AuNCs@MUA increases from ~1.9 nm to ~2.1 nm in presence of FA, also indicating the formation of complex.

3.3 Optimization of parameters in sensing FA

In order to detect FA under suitable conditions, several factors affecting the ratio of fluorescence intensity (I_{446}/I_{612}) are optimized such as pH value, reaction time, concentration of probe and buffer systems. As shown in Fig. 3a, the I_{446}/I_{612} of AuNCs@MUA-FA system demonstrates strong response toward the target over the pH of 6–9 while except for the acidic (pH < 6) and strongly alkaline (pH > 10) conditions. Clearly, this special response toward pH value should be ascribed to chemical properties of FA, which is more stable in neutral and weak basic conditions.[37] Next, the fluorescence response of the concentration of AuNCs@MUA is investigated in Fig. 3b. In presence of FA with given concentration, it is clear to find that I_{446}/I_{612} decreases linearly as increasing the concentration of AuNCs@MUA from 5 to 25 μM. Considering the effect of signal-to-noise ratio, we use 10 μM AuNCs@MUA in the following detection procedure. Additionally, the effects of buffer systems and reaction time are shown in Fig. 3c and d, respectively. Results show the Tris buffer is more suitable to detection and reaction is fairly fast, which reaches equilibrium in less than 2 min.

3.4 Ratiometric fluorescence detection of FA

Under optimum conditions, the fluorescence response of AuNCs@MUA-FA system is record by adding increasing amounts of FA (0–20 μM) into AuNCs@MUA (10 μM) contained Tris buffer solution (pH = 8). As shown in Fig. 4a, the ratio I_{446}/I_{612} is proportional to the concentration of FA. The linear range of AuNCs@MUA toward FA is from 0 to 20 μM with a good correlation coefficient of 0.9992 (Fig. 4b). Besides, the limit of detection (LOD) is estimated as 26 nM at a signal-to-noise ratio of 3. As shown in Table S1,† it is evident to see that the LOD is comparable to other reported fluorescence probes, suggesting this platform is sensitive and reliable for FA detection.

3.5 Interference of coexisting substance

To evaluate the possible effect originated from biochemicals or ions in physiological circumstances on sensing FA, various substance such as glucose, BSA, amino acids, and K^+, Na^+, Mg^{2+}, Ca^{2+}, Cl^-, CO_3^{2-}, HCO_3^-, PO_4^{3-}, HPO_4^{2-}, $H_2PO_4^-$ are separately introduced into the current detection procedures. As indicated in Fig. 4c and d, these biochemical molecules and ions show scarce effect on the fluorescence intensity ratio of the designed assay, suggesting its acceptable endurance for interference.

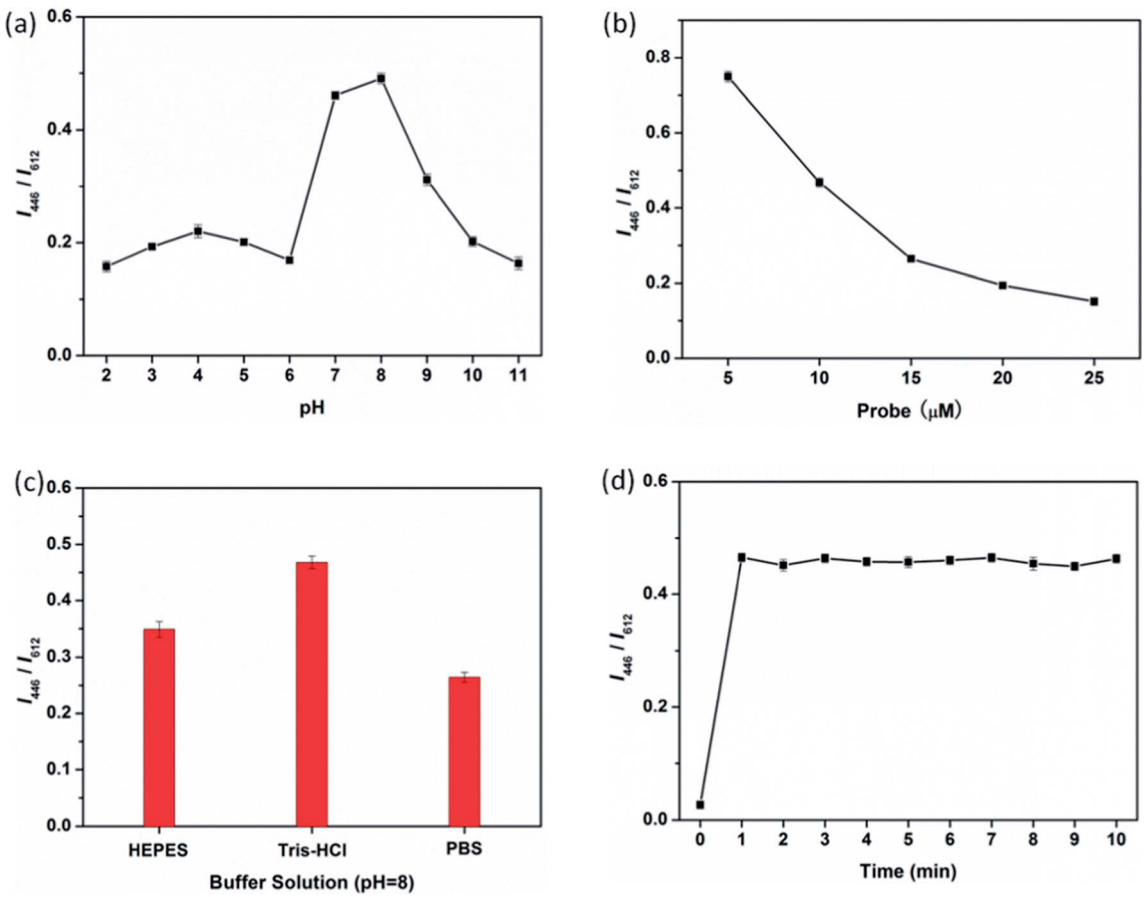

Fig. 3 (a) pH, (b) concentration, (c) buffer systems, and (d) time dependent fluorescence response upon addition of FA (20 μM).

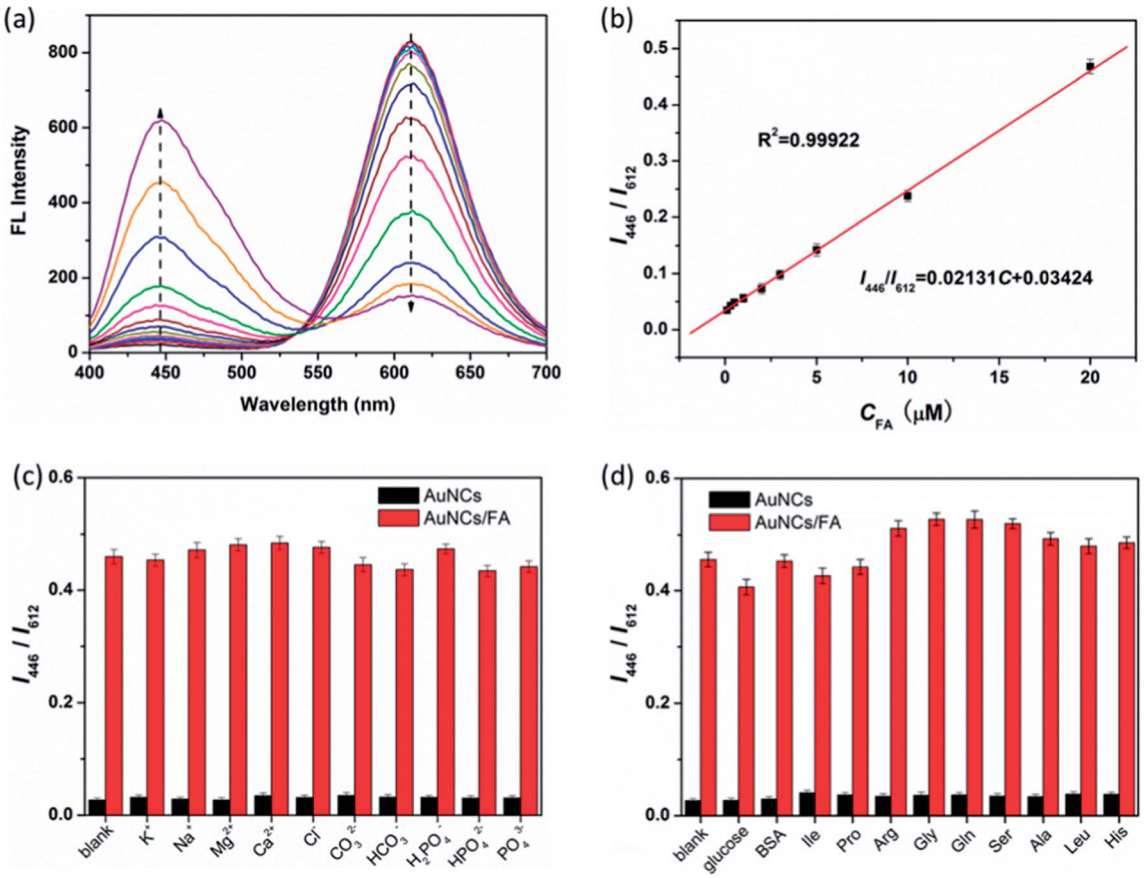

Fig. 4 (a) Fluorescence emission spectra of AuNCs@MUA-FA system upon addition of different concentrations of FA (0, 0.1, 0.3, 0.5, 1, 2, 3, 5, 10, 20, 50, 100, 200 μM). (b) Linear relationships between I_{446}/I_{612} and the concentrations of FA from 0 to 20 μM. Relative fluorescence intensity (I_{446}/I_{612}) of AuNCs@MUA after adding (c) ions and (d) biological agents (BSA, glucose and amino acids) in the absence or presence of FA.

3.6 Detection in real sample

To further evaluate the practicality of this developed system, the AuNCs@MUA are used to detect FA in spiked human serum samples. We measure and calculate recovery rate and relative standard deviation (RSD) to evaluate accuracy of the detection. The recovery rate is defined as $(A/B) \times 100\%$, where the A and B are respectively measured and actual concentration of FA; while the RSD can be obtained by the equation

$$\mathrm{RSD} = \frac{\mathrm{SD}}{\bar{x}} \times 100\% = \sqrt{\frac{\sum_{i=1}^{n}(x_i - \bar{x})^2}{n-1}} \Bigg/ \frac{\sum_{i=1}^{n} x_i}{n} \times 100\% \quad (2)$$

Table 1 Determination of FA in human serum samples

Samples	Added (μM)	Found (μM)	Recovery (%)	RSD ($n = 3$, %)
1#	0	0	—	—
2#	1.00	1.02	102	3.6
3#	2.00	1.91	95.4	4.2
4#	5.00	4.87	97.4	2.7

where SD and $\bar{x}$ represent standard deviation and average of measurements, respectively. As listed in Table 1, the recoveries range from 95.4% to 102% in human serum samples and all the RSD are lower than 4.2%, definitely suggesting the accuracy and reliability of the present radiometric fluorescence strategy for detecting FA levels in human serum samples.

4. Conclusion

In summary, we demonstrate a novel ratiometric fluorescence platform for detection of FA by using AuNCs@MUA. Such strategy can monitor FA *via* the changes of dual-emission florescence, one is quenching of AuNCs@MUA and the other is auto-florescence enhancement of FA. In comparison to previous probes with single fluorescence, this platform possesses many advantages such as dual-emission responses, strong anti-interference toward target, well biocompatibility and high sensitivity. Moreover, this ratiometric fluorescence system doesn't need any further crosslinking or modifications after preparation of AuNCs@MUA, making it cost-effective. The current efforts perform an important step to further design of the platform toward FA with dual-emission response, which greatly extends the potential of FA detection in practical applications.

Conflicts of interest

There are no conflicts to declare.

Acknowledgements

This work are financially supported by Programs of Jilin Department of Science and Technology (No. 20180520006JH, 20180520161JH), Jilin Department of Education (JJKH20170213KJ, JJKH20170216KJ), and Jilin Technology Bureau (201750258, 20166021).

Notes and references

1 B. A. Lashner, K. S. Provencher, D. L. Seidner, A. Knesebeck and A. Brzezinski, *Gastroenterology*, 1997, **112**, 29–32.
2 S. Wei, F. Zhao, Z. Xu and B. Zeng, *Microchim. Acta*, 2006, **152**, 285–290.
3 Y. I. Kim, *J. Nutr. Biochem.*, 1999, **10**, 66–88.
4 A. Lermo, S. Fabiano, S. Hernández, R. Galve, M. P. Marco, S. Alegret and M. I. Pividori, *Biosens. Bioelectron.*, 2009, **24**, 2057–2063.
5 S. N. Young, *Can. J. Physiol. Pharmacol.*, 1991, **69**, 893–903.
6 Y. Wang, J. Zheng, Z. Zhang, C. Yuan and D. Fu, *Colloids Surf., A*, 2009, **342**, 102–106.
7 D. Hoegger, P. Morier, C. Vollet, D. Heini, F. Reymond and J. S. Rossier, *Anal. Bioanal. Chem.*, 2007, **387**, 267–275.
8 S. Zhao, H. Yuan, C. Xie and D. Xiao, *J. Chromatogr. A*, 2006, **1107**, 290–293.
9 D. E. Breithaupt, *Food Chem.*, 2001, **74**, 521–525.
10 E. Gujska and A. Kuncewicz, *Eur. Food Res. Technol.*, 2005, **221**, 208–213.
11 A. Rodríguez-Bernaldo de Quirós, C. Castro de Ron, J. López-Hernández and M. A. Lage-Yusty, *J. Chromatogr. A*, 2004, **1032**, 135–139.
12 F. Xiao, C. Ruan, L. Liu, R. Yan, F. Zhao and B. Zeng, *Sens. Actuators, B*, 2008, **134**, 895–901.
13 Z. J. Sun, Z. W. Jiang and Y. F. Li, *RSC Adv.*, 2016, **6**, 79805–79810.
14 W. Ren, Y. Fang and E. Wang, *ACS Nano*, 2011, **5**, 6425–6433.
15 J. Das Sarma, C. Duttagupta, E. Ali and T. K. Dhar, *J. Immunol. Methods*, 1995, **184**, 1–6.
16 X. Li, X. Tan, J. Yan, Q. Hu, J. Wu, H. Zhang and X. Chen, *Electrochim. Acta*, 2016, **187**, 433–441.
17 H. Dai, Y. Li, S. Zhang, L. Gong, X. Li and Y. Lin, *Sens. Actuators, B*, 2016, **222**, 120–126.
18 S. Kundu, S. Maiti, T. K. Das, D. Ghosh, C. N. Roy and A. Saha, *Analyst*, 2017, **142**, 2491–2499.
19 M. Wang, Y. Jiao, C. Cheng, J. Hua and Y. Yang, *Anal. Bioanal. Chem.*, 2017, **409**, 7063–7075.
20 P. Liu, D. Liu, Y. Liu and L. Li, *J. Solid State Chem.*, 2017, **241**, 164–172.
21 A. A. Ensafi, P. Nasr-Esfahani and B. Rezaei, *Anal. Chim. Acta*, 2017, **996**, 64–73.
22 X. Yan, H. Li, B. Cao, Z. Ding and X. Su, *Microchim. Acta*, 2015, **182**, 1281–1288.
23 B. Hemmateenejad, F. Shakerizadeh-shirazi and F. Samari, *Sens. Actuators, B*, 2014, **199**, 42–46.
24 I. A. Mir, K. Rawat, P. R. Solanki and H. B. Bohidar, *J. Nanopart. Res.*, 2017, **19**, 260.
25 S. Chakravarty, P. Dutta, S. Kalita and N. Sen Sarma, *Sens. Actuators, B*, 2016, **232**, 243–250.
26 J. Sun, J. Zhang and Y. Jin, *J. Mater. Chem. C*, 2013, **1**, 138–143.
27 S. Liu, J. Hu and X. Su, *Analyst*, 2012, **137**, 4598–4604.
28 S. Liu, F. Shi, L. Chen and X. Su, *Microchim. Acta*, 2014, **181**, 339–345.
29 Z. Wu, M. Wang, J. Yang, X. Zheng, W. Cai, G. Meng, H. Qian, H. Wang and R. Jin, *Small*, 2012, **8**, 2028–2035.
30 J. Sun, F. Yang and X. Yang, *Nanoscale*, 2015, **7**, 16372–16380.
31 W. P. Hu, S. J. Chen, K. T. Huang, J. H. Hsu, W. Y. Chen, G. L. Chang and K. A. Lai, *Biosens. Bioelectron.*, 2004, **19**, 1465–1471.
32 M. Kubista, R. Sjoback, S. Eriksson and B. Albinsson, *Analyst*, 1994, **119**, 417–419.
33 R. M. Clegg, *Curr. Opin. Biotechnol.*, 1995, **6**, 103–110.
34 W.-J. Niu, D. Shan, R.-H. Zhu, S.-Y. Deng, S. Cosnier and X.-J. Zhang, *Carbon*, 2016, **96**, 1034–1042.
35 Y. Qin, Y. Zhang, S. Yan and L. Ye, *Spectrochim. Acta, Part A*, 2010, **75**, 1506–1510.
36 S. Mohapatra, S. K. Mallick, T. K. Maiti, S. K. Ghosh and P. Pramanik, *Nanotechnology*, 2007, **18**, 385102.
37 R. Matias, P. R. S. Ribeiro, M. C. Sarraguca and J. A. Lopes, *Anal. Methods*, 2014, **6**, 3065–3071.